Singularity Avoidance/Passage Steering Logic for a Variable-speed Double-gimbal Control Moment Gyro Based on Inverse Kinematics

By Shota KAWAJIRI,[1)] and Saburo MATUNAGA[2)]

[1)] *Department of Mechanical and Aerospace Engineering, Tokyo Institute of Technology, Tokyo, Japan*
[2)] *Department of Mechanical Engineering, Tokyo Institute of Technology, Tokyo, Japan*

(Received June 21st, 2017)

In this paper, we propose a novel singularity avoidance/passage logic based on inverse kinematics for steering a variable-speed double-gimbal control moment gyro. This method does not employ any correction term, which is for the singularity avoidance and required in a previously proposed steering logic, and it can generate a precise torque close to the reference torque. Also, it uses an evaluation function including gimbal rate limitations explicitly for singularity avoidance/passage decision. Its function leads a decision causing small attitude-error compared with the previous method which uses a simple threshold. Effectiveness of the method is demonstrated by numerical simulations.

Key Words: Attitude Control, Control Moment Gyro, Double Gimbal, Variable Wheel Speed

Nomenclature

$\vec{b}_i$	:	ith axis of the body fixed coordinate ($i = 1, 2, 3$)
$\boldsymbol{h}$	:	angular momentum
h_W	:	magnitude of the wheel angular velocity
$\boldsymbol{J}$	:	inertia matrix of a spacecraft
Δt	:	control period of attitude control
$\boldsymbol{\omega}$	:	body angular velocity
θ	:	gimbal angle of a VSDGCMG
$\boldsymbol{\tau}$	:	output torque
Subscripts		
I	:	inner gimbal
O	:	outer gimbal
ref	:	reference
t	:	total
W	:	wheel
Superscripts		
$+$	:	solution when $\cos(\theta_I + \Delta\theta_I) > 0$
$-$	:	solution when $\cos(\theta_I + \Delta\theta_I) < 0$
$*$	:	numerically integrated values

Bold letters denote elements in the body fixed coordinate unless otherwise stated.

1. Introduction

Recently, many challenging space missions for science and engineering have been carried out by using micro satellites, which can be developed at low cost in a short time. Examples of those micro satellites are a 50 kg class micro satellite "TSUBAME"[1)] developed at Tokyo Institute of Technology, and a small deep space probe "PROCYON"[2)] developed at The University of Tokyo and JAXA. One of the problems regarding micro satellites is their small volume and this requires a device installed on a satellite to be small size. For the problem, using a variable-speed double-gimbal control moment gyro (VSDGCMG) for three-axis attitude control is a promising option and expected to be able to save more space than using three reaction wheels. This is because the actuator has three degrees of freedom per one device and three-axis attitude control can be conducted by only one VSDGCMG.

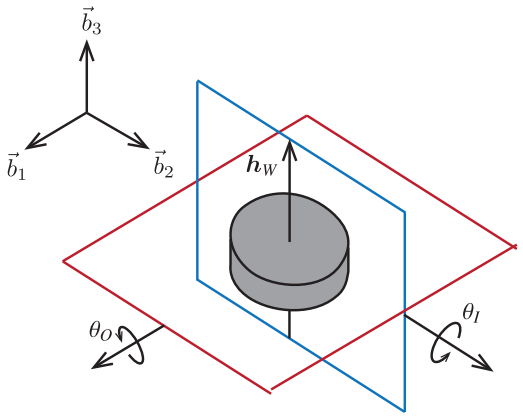

Fig. 1.: VSDGCMG configuration when $\theta_i = \theta_o = 0$.

The mechanics of the VSDGCMG is shown as Fig. 1. The CMG consists of a wheel and two gimbal: an inner gimbal and an outer gimbal. The variable-speed wheel rotates at high speed in a spacecraft and the inner gimbal rotates the wheel around an axis orthogonal to the wheel's rotation-axis. The outer gimbal further rotates the inner gimbal around an axis orthogonal to the outer gimbal axis.

Several attitude control methods using a VSDGCMG has been proposed: a non-linear control method derived from a strict equation of motion,[3)] a backstepping control method,[4)] and a time-optimal maneuver planning method.[5)] However, few studies focus on a singular problem where the CMG sometimes cannot generate torque along a certain direction. The singular states of the VSDGCMG can be divided into two types: 1) the wheel speed becomes zero and 2) the wheel's rotational axis coincides with the outer gimbal axis. Tsukahara et al. proposed a steering logic[6)] to avoid and pass the latter singular state. The avoidance means not being trapped at the state and the passage means leaving from the singularity after being trapped. When

an approximate variation of the outer gimbal angle in the vicinity of the singular state is larger than a threshold, the singularity avoidance is conducted. The passage is conducted when the variation is small.

In this paper, first, we propose a singularity avoidance steering logic by modifying the IKSL[7] (inverse kinematics steering logic) for a VSDGCMG. Then, we show that this singlarity avoidance logic causes large attitude error due to the considerable increase of the reference gimbal rate in the vicinity of the singular state. Second, we propose a singularity avoidance/passage steering logic to prevent the error.

The inverse kinematics is a method to obtain magnitude of each wheel momentum and each gimbal angle from angular momentum of a CMG system. Using the inverse kinematics makes a correction term unnecessary, which is used for avoiding the singular state in the steering logic derived from dynamics. Also, the usage makes the CMG system generate torque close to commanded value. In particular, applying the inverse kinematics to the VSDGCMG is reasonable because the magnitude of the wheel momentum and the two gimbal angles can be easily calculated from the CMG momentum. Compared with the Tsukahara's method, the proposed singularity avidance/passage logic has a characteristic that an evaluation function for the singularity avoidance/passage decision explicitly includes gimbal rate limitations. Essentially, the avoidance/passage decision depends on the gimbal rate limitations; if there is no limitation, the avoidance should be always conducted. Therefore, the proposed method including the limitations explicitly can decide more appropriately (with smaller attitude-error) than the previous one can.

In section 2 of the paper, a mathematical model of a spacecraft with a VSDGCMG is described. In section 3, the steering logic based on the inverse kinematics is proposed. In section 4, effectiveness of the proposed method is demonstrated by numerical simulations. We present our conclusions in section 5.

2. Mathematical model

Total angular momentum of a spacecraft with a VSDGCMG can be approximated as follows.

$$\boldsymbol{h}_t = \boldsymbol{J}\boldsymbol{\omega} + \boldsymbol{h}_W \tag{1}$$

We assume a configuration that the outer gimbal axis, the inner gimbal axis and the wheel axis coincide with each axis of the body fixed coordinate when $\theta_I = \theta_O = 0$ as shown in the Fig. 1. In the configuration, the wheel angular momentum $\boldsymbol{h}_W$ is expressed in the body fixed coordinate as

$$\boldsymbol{h}_W(\boldsymbol{\theta}, h_W) = h_W \begin{bmatrix} \sin\theta_I \\ -\sin\theta_O \cos\theta_I \\ \cos\theta_O \cos\theta_I \end{bmatrix} \tag{2}$$

where $\boldsymbol{\theta} = [\theta_O \ \theta_I]^T$.

By taking the time derivative in the inertial coordinate, we can obtain the following equation of motion.

$$\boldsymbol{J}\dot{\boldsymbol{\omega}} + \boldsymbol{\omega} \times \boldsymbol{h}_t = \boldsymbol{B}\boldsymbol{u} \tag{3}$$

$\boldsymbol{B}\boldsymbol{u}$ is a time derivative of the wheel angular momentum in the body fixed coordinate and expressed as follows.

$$\boldsymbol{B} = \begin{bmatrix} 0 & -h_W \cos\theta_I & -\sin\theta_I \\ h_W \cos\theta_O \cos\theta_I & -h_W \sin\theta_O \sin\theta_I & \sin\theta_O \cos\theta_I \\ h_W \sin\theta_O \cos\theta_I & h_W \cos\theta_O \sin\theta_I & -\cos\theta_O \cos\theta_I \end{bmatrix} \tag{4}$$

$$\boldsymbol{u} = \begin{bmatrix} \dot{\theta}_O & \dot{\theta}_I & \dot{h}_W \end{bmatrix}^T \tag{5}$$

As is clear from the jacobian matrix $\boldsymbol{B}$, there are two singular states: $\cos\theta_I = 0$ and $h_W = 0$. In the former case, the wheel axis coincides with the outer gimbal axis and the output torque lies in a two-dimensional plane; the torque cannot point to an arbitrary direction. In the latter case, the wheel rotation stops. In this paper, we focus on the former singular state which the CMG is likely to encounter during attitude maneuvers.

3. Proposed method

For a VSDGCMG, IKSL calculates control inputs $\dot{h}_W$ and $\dot{\boldsymbol{\theta}} = [\dot{\theta}_O \ \dot{\theta}_I]^T$ as follows. It calculates reference angular momentum $\boldsymbol{h}_{W\mathrm{ref}} = \boldsymbol{h}_W(\boldsymbol{\theta}_{\mathrm{ref}}, h_{W\mathrm{ref}})$, which the CMG should have after a sufficiently small control period Δt, from a given reference output torque $\boldsymbol{\tau}_{\mathrm{ref}}$ and the current angular momentum $\boldsymbol{h}_W$. To possess the reference momentum $\boldsymbol{h}_{W\mathrm{ref}}$, the reference wheel-momentum magnitude $h_{W\mathrm{ref}}$ and the reference gimbal angles $\boldsymbol{\theta}_{\mathrm{ref}}$ are calculated. Finally, the control inputs $\dot{h}_W$ and $\dot{\boldsymbol{\theta}}$ are determined such that the wheel-momentum magnitude and the gimbal angles vary by $\Delta h (= h_{W\mathrm{ref}} - h_W)$ and $\Delta\boldsymbol{\theta} (= \boldsymbol{\theta}_{\mathrm{ref}} - \boldsymbol{\theta})$ during Δt, respectively.

Given the reference torque and the current CMG momentum, time derivative of the CMG momentum should be as follows.

$$\frac{\mathrm{d}\boldsymbol{h}_W}{\mathrm{d}t} = -\boldsymbol{\tau}_{\mathrm{ref}} \tag{6}$$

A first-order approximation leads the following reference momentum.

$$\boldsymbol{h}_{W\mathrm{ref}} = \boldsymbol{h}_W - \boldsymbol{\tau}_{\mathrm{ref}}\Delta t \tag{7}$$

Substituting $\boldsymbol{h}_{W\mathrm{ref}} = \boldsymbol{h}_W(\boldsymbol{\theta}_{\mathrm{ref}}, h_{W\mathrm{ref}})$ and the Eq. (2) into the Eq. (7), we can obtain the following equation.

$$h_{W\mathrm{ref}} \begin{bmatrix} \sin\theta_{I\mathrm{ref}} \\ -\sin\theta_{O\mathrm{ref}} \cos\theta_{I\mathrm{ref}} \\ \cos\theta_{O\mathrm{ref}} \cos\theta_{I\mathrm{ref}} \end{bmatrix} = \boldsymbol{h}_W - \boldsymbol{\tau}_{\mathrm{ref}}\Delta t \tag{8}$$

By representing the right-hand side of the equation above as $[h_1 \ h_2 \ h_3]^T$, the equations to be solved become as follows.

$$h_{W\mathrm{ref}} \sin\theta_{I\mathrm{ref}} = h_1 \tag{9}$$

$$-h_{W\mathrm{ref}} \sin\theta_{O\mathrm{ref}} \cos\theta_{I\mathrm{ref}} = h_2 \tag{10}$$

$$h_{W\mathrm{ref}} \cos\theta_{O\mathrm{ref}} \cos\theta_{I\mathrm{ref}} = h_3 \tag{11}$$

Sum of squares of the Eq. (9) – (11) leads the following equation.

$$h_{W\mathrm{ref}}^2 = h_1^2 + h_2^2 + h_3^2 \tag{12}$$

Square root of the sum of squares of the Eq. (10) and the Eq. (11) becomes:

$$h_{W\mathrm{ref}} \cos\theta_{I\mathrm{ref}} = \pm\sqrt{h_2^2 + h_3^2} \tag{13}$$

Now, we assume that $h_{W\mathrm{ref}} \neq 0$ and $h_2^2 + h_3^2 \neq 0$. Dividing the Eq. (9) by the equation above leads the following equation.

$$\theta_{I\mathrm{ref}} = \tan^{-1} \frac{h_1}{\pm\sqrt{h_2^2 + h_3^2}} \tag{14}$$

Substituting the equation above into the Eq. (10) and (11), we obtain

$$\mp\sqrt{h_2^2 + h_3^2} \sin\theta_{O\mathrm{ref}} = h_2 \tag{15}$$

$$\pm\sqrt{h_2^2 + h_3^2} \cos\theta_{O\mathrm{ref}} = h_3 \tag{16}$$

Dividing the Eq. (15) by the Eq. (16) leads the following equation.

$$\theta_{O\mathrm{ref}} = \begin{cases} \tan^{-1}\frac{-h_2}{h_3} & (\cos\theta_{I\mathrm{ref}} > 0) \\ \tan^{-1}\frac{h_2}{-h_3} & (\cos\theta_{I\mathrm{ref}} < 0) \end{cases} \tag{17}$$

Using $\Delta h = h_{W\mathrm{ref}} - h_W$ and $\Delta\boldsymbol{\theta} = \boldsymbol{\theta}_{\mathrm{ref}} - \boldsymbol{\theta}$, we can summarize the solution of the Eq. (8) as

$$\Delta h_W = -h_W + \sqrt{h_1^2 + h_2^2 + h_3^2} \tag{18}$$

$$\Delta\theta_I = -\theta_I + \tan^{-1} \frac{h_1}{\pm\sqrt{h_2^2 + h_3^2}} \tag{19}$$

$$\Delta\theta_O = \begin{cases} -\theta_O + \tan^{-1}\frac{-h_2}{h_3} & (\cos\theta_{I\mathrm{ref}} > 0) \\ -\theta_O + \tan^{-1}\frac{h_2}{-h_3} & (\cos\theta_{I\mathrm{ref}} < 0) \end{cases} \tag{20}$$

Although two solutions exist, either should be selected such that the sign of $\cos\theta_{I\mathrm{ref}}$ equals that of $\cos\theta_I$. As $h_2^2 + h_3^2$ seldom strictly becomes zero on the computer, this selection can avoid being trapped into (numerically diverging near) the singular state of $\cos\theta_{I\mathrm{ref}} = 0$ without a correction term required in the dynamics-based steering logic. Also, the absence of the correction-term makes the output-torque close to the reference. Now, we distinguish the two solutions by superscripts + and − which denote signs of $\cos\theta_{I\mathrm{ref}}$. Using this notation, the Eq. (19) and (20) show the following relationship.

$$\theta^-_{I\mathrm{ref}} + \theta^+_{I\mathrm{ref}} = \begin{cases} \pi & (\sin\theta^+_{I\mathrm{ref}} > 0) \\ -\pi & (\sin\theta^+_{I\mathrm{ref}} < 0) \end{cases} \tag{21}$$

$$\theta^-_{O\mathrm{ref}} - \theta^+_{O\mathrm{ref}} = \pi \tag{22}$$

It is found that two solutions of $\theta_{I\mathrm{ref}}$ approach each other in the vicinity of $\cos\theta^+_{I\mathrm{ref}} = 0$ and those of $\theta_{O\mathrm{ref}}$ always differs by π radians. If $h_{W\mathrm{ref}} \neq 0$ and $h_2^2 + h_3^2 = 0$, the following solution is selected.

$$\Delta h_W = -h_W + \sqrt{h_1^2 + h_2^2 + h_3^2} \tag{23}$$

$$\Delta\theta_I = -\theta_I \pm \pi/2 \tag{24}$$

$$\Delta\theta_O = 0 \tag{25}$$

For $h_{W\mathrm{ref}} = 0$, a selected solution is as follows.

$$\Delta h_W = -h_W \tag{26}$$

$$\Delta\theta_I = 0 \tag{27}$$

$$\Delta\theta_O = 0 \tag{28}$$

Again, as $h_2^2 + h_3^2$ seldom strictly becomes zero on the computer and we focus on $h_{W\mathrm{ref}} > 0$, the Eq. (18) – (20) are mainly used.

Using the result of the inverse kinematics, control inputs can be obtained as follows.

$$\dot{\boldsymbol{h}}_W = \frac{\Delta h_W}{\Delta t}, \quad \dot{\boldsymbol{\theta}} = \frac{\Delta\boldsymbol{\theta}}{\Delta t} \tag{29}$$

We analyze behavior of the outer gimbal angle in the vicinity of the singular state of $\cos\theta_I = 0$ when the proposed steering logic is employed. For an example, the case is studied where the state keeping $\cos\theta_I > 0$ approaches to the singularity. Substituting the Eq. (2) and (7) into the Eq. (20), we obtain

$$\Delta\theta_O = -\theta_O + \tan^{-1} \frac{h_W \sin\theta_O \cos\theta_I + \tau_2\Delta t}{h_W \cos\theta_O \cos\theta_I - \tau_3\Delta t} \tag{30}$$

where τ_i is a ith ($i = 1, 2, 3$) element of $\boldsymbol{\tau}_{\mathrm{ref}}$. Substituting the Eq. (29) into the Eq. (30) and approximating that $\cos\theta_I \approx 0$, we can obtain the following differential equation.

$$\dot{\theta}_O(t) = \frac{1}{\Delta t}\left(-\theta_O(t) + \tan^{-1}\frac{\tau_2(t)}{-\tau_3(t)}\right) \tag{31}$$

Furthermore, assuming that the time-period when the state is in the vicinity of the singularity is sufficiently short and the reference torque $\boldsymbol{\tau}_{\mathrm{ref}}$ can be regarded as constant in the period, we can easily solve the equation as

$$\theta_O(t) = (\theta_O(0) - C)\exp\left(-\frac{t}{\Delta t}\right) + C \tag{32}$$

where $C = \tan^{-1}(\tau_2/-\tau_3)$. This solution shows that θ_O approaches to C as time passes. If we rewrite the Eq. (31) using the Eq. (32), the following equation can be obtained.

$$\dot{\theta}_O(t) = \frac{-1}{\Delta t}(\theta_O(0) - C)\exp\left(-\frac{t}{\Delta t}\right) \tag{33}$$

This equation shows that the norm of the control input $|\dot{\theta}_O|$ reaches a maximum value of $|(\theta_o(0) - C)/\Delta t|$ in the vicinity of the singular state. The value may violate gimbal rate limitations which the general CMG has and the violation can cause large attitude error.

To avoid the attitude error, we consider a method to pass the singular state (once pass $\cos\theta_I = 0$ and escape from there) and then we propose a novel singularity avoidance/passage steering logic. For an example, the case is studied where we select the $\boldsymbol{\theta}^+_{\mathrm{ref}}$ solution, $\theta_O(0) = 0$ and $C^+ = \pi$ [rad]. In the case, $C^- = 0$ and the $\boldsymbol{\theta}^-_{O\mathrm{ref}}$ solution approaches the initial gimbal angle $\theta_O(0) = 0$ as time passes. Therefore, when the control input far exceeds the upper limit near the singularity, changing the selected solution to $\theta^-_{O\mathrm{ref}}$ seems to be able to decrease more attitude error than continuing to select the $\theta^+_{O\mathrm{ref}}$ solution as shown in the Fig . 2. When using the method, we must select θ^-_{Iref} too. This "transition" regarding the inner gimbal angle is expected to have less impact on the attitude because the Eq. (21) leads $\theta^+_I \approx \pm\pi/2$ and $\theta^-_I \approx \pm\pi/2$ in the vicinity of the singular state as shown in Fig . 3. Hereinafter, we mention how to decide whether to transit, and the control inputs during the transition. For simplicity, we consider the case where $\cos\theta_I$ changes from positive to negative across $\pi/2$ radians.

As an evaluation function $L(\Delta\boldsymbol{\theta}, \Delta h_W)$ to decide whether the algorithm transitions to the another solution, we employ "the difference between the average torque during T_1 and the torque $-\boldsymbol{\tau}_{\mathrm{ref}}$ which the CMG should be affected from the spacecraft

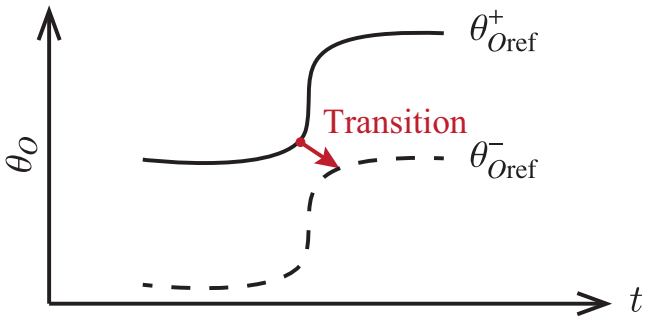

Fig. 2.: Transition of the solution for the outer gimbal angle θ_o.

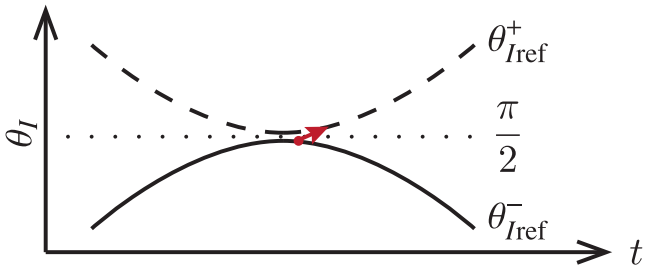

Fig. 3.: Transition of the solution for the inner gimbal angle θ_I.

during that time by changing the gimbal angles and the wheel speed":

$$L(\Delta\boldsymbol{\theta}, \Delta h_W) = \left| \left\{ \boldsymbol{h}_W \left(\underset{\boldsymbol{\theta}+\dot{\boldsymbol{\theta}}_{\max} T_1, \boldsymbol{\theta}+\dot{\boldsymbol{\theta}}_{\min} T_1}{\text{sat}} (\boldsymbol{\theta} + \Delta\boldsymbol{\theta}), h_W + \Delta h_W^* \right) - \boldsymbol{h}_W(\boldsymbol{\theta}, h_W) \right\} / T_1 + \boldsymbol{\tau}_{\text{ref}} \right| \tag{34}$$

where $\dot{\boldsymbol{\theta}}_{\max}$ and $\dot{\boldsymbol{\theta}}_{\min}$ are gimbal-rate upper and lower limitations, respectively, and "sat" denotes a saturation function defined as

$$\underset{\theta_{\max}, \theta_{\min}}{\text{sat}} (\theta) = \begin{cases} \theta_{\max} & (\theta > \theta_{\max}) \\ \theta & (\theta_{\min} \le \theta \le \theta_{\max}) \\ \theta_{\min} & (\theta < \theta_{\min}) \end{cases} \tag{35}$$

The evaluation function about selecting $\boldsymbol{\theta}_{\text{ref}}^{+}$ and $\boldsymbol{\theta}_{\text{ref}}^{-}$ becomes as follows, respectively.

$$L^{+} = L(\Delta\boldsymbol{\theta}^{*+}, \Delta h_W^*) \tag{36}$$

$$L^{-} = L(\Delta\boldsymbol{\theta}^{*-}, \Delta h_W^*) \tag{37}$$

where $\Delta\boldsymbol{\theta}^*$ and Δh_W^* are integrated values calculated by using the Eq. (18)–(20) from the current time t to $t+T_1$. The reference torque $\boldsymbol{\tau}_{\text{ref}}$ is assumed to be constant at the current reference torque during the integration.

As the evaluation function includes the gimbal rate limitation explicitly, the proposed method can decide more appropriately than the previous one can. If $L^+ > L^-$ and the minimum value of $|\cos\theta_I|$ during T_1, which is denoted as $|\cos\theta_I|_{\min}$, is less than ε, the transition starts. During the time-period of T_2 for the transition, the control inputs are selected as follows.

$$\dot{\theta}_O = \underset{\dot{\theta}_{\max}, \dot{\theta}_{\min}}{\text{sat}} \left(\frac{1}{\Delta t} \frac{t}{T_2} (\theta_O^- - \theta_O) \right) \tag{38}$$

$$\dot{\theta}_I = \underset{\dot{\theta}_{\max}, \dot{\theta}_{\min}}{\text{sat}} \left(\frac{1}{\Delta t} \frac{t}{T_2} (\theta_I^- - \theta_I) \right) \tag{39}$$

Although there is a large difference between the reference angles $\boldsymbol{\theta}_{\text{ref}}^{-}$ and the current angles $\boldsymbol{\theta}$ at the start time of the transition, the reference approaches to the current as time passes; therefore, the inputs are designed such that the current values $\boldsymbol{\theta}$ gradually approach to the reference $\boldsymbol{\theta}_{\text{ref}}^{-}$ because

Summarizing the above, the singularity avoidance/passage steering logic is conducted as follows.

1. Integrate gimbal angle and wheel angular momentum using the Eq. (18)–(20) during T_1.
2. If $L^+ > L^-$ and $|\cos\theta_i|_{\min} < \varepsilon$ hold true, go to 3. If not, go to 4.
3. Steering the gimbals using the Eq. (38) and (39) during T_2. Then, go to 1.
4. Steering the gimbals using the Eq. (18)–(20) or the Eq. (23)–(28). Then, go to 1.

4. Numerical simulations

Numerical simulations are carried out to verify the validity and effectiveness of the proposed method, where the attitude and the angular velocity track the pre-defined trajectories. Based on the Ref. 6), parameters common to the all simulations are specified as

$$\boldsymbol{J} = \text{diag}\begin{bmatrix} 3.41 & 2.89 & 2.55 \end{bmatrix} [\text{kgm}^2]$$

$$\boldsymbol{\omega}_{\text{ref}} = \begin{cases} \frac{t}{14}\boldsymbol{\omega}_f & 0 \le t < 14 \\ \boldsymbol{\omega}_f & 14 \le t < 16 \\ \frac{30-t}{30}\boldsymbol{\omega}_f & 16 \le t \le 30 \end{cases}$$

$$\theta_O(0) = -\pi/4[\text{rad}], \quad \theta_I(0) = 1.36[\text{rad}], \quad h_W(0) = 0.1[\text{Nms}]$$

$$T_1 = 1.0[\text{sec}], \quad T_2 = 2.0[\text{sec}], \quad \varepsilon = 0.1$$

$$\dot{\theta}_{\max} = 1[\text{rad/s}], \quad \dot{\theta}_{\min} = -1[\text{rad/s}]$$

where $\boldsymbol{\omega}_{\text{ref}}$ is the reference angular velocity and has the trapezoidal trajectory. The reference quaternion is calculated by integrating the reference angular velocity. The reference torque is calculated as

$$\boldsymbol{\tau}_{\text{ref}} = \boldsymbol{J}\dot{\boldsymbol{\omega}}_{\text{ref}} + \boldsymbol{\omega} \times \boldsymbol{h}_t + k_\omega \boldsymbol{\omega}_{\text{err}} + k_q V(\boldsymbol{q}_{\text{err}}) \tag{40}$$

where $k_\omega = 5.0$ and $k_q = 1.25$. $\boldsymbol{q}_{\text{err}}$ is the error quaternion between the current and the reference attitude. $V(\boldsymbol{q})$ is a function which returns the part of the quaternion ($V(\boldsymbol{q}) = [q_1 \; q_2 \; q_3]^T$). $\boldsymbol{\omega}_{\text{err}}$ is error angular velocity and defined as follows.

$$\boldsymbol{\omega}_{\text{err}} = \boldsymbol{\omega} - \boldsymbol{\omega}_{\text{ref}} \tag{41}$$

We specified the Euler method as the numerical integration conducted in the steering logic. This is because the method has the advantage in the low computational complexity and it can be calculated even on an on-board computer. The integration time is 0.1 s. As for the initial value of the inner and outer gimbal angle, we specified the angle in the vicinity of the singular state, and the angle which is difficult to generate torque along +YZ direction, respectively.

Three cases are carried out where reference angular velocity differs as follows.

- Case A: $\boldsymbol{\omega}_f = 0.02\sqrt{0.5}\begin{bmatrix} 0 & 1 & 1 \end{bmatrix}^T$ [rad/s]
- Case B: $\boldsymbol{\omega}_f = 0.028\sqrt{0.5}\begin{bmatrix} 0 & 1 & 1 \end{bmatrix}^T$ [rad/s]
- Case C: $\boldsymbol{\omega}_f = 0.04\sqrt{0.5}\begin{bmatrix} 0 & 1 & 1 \end{bmatrix}^T$ [rad/s]

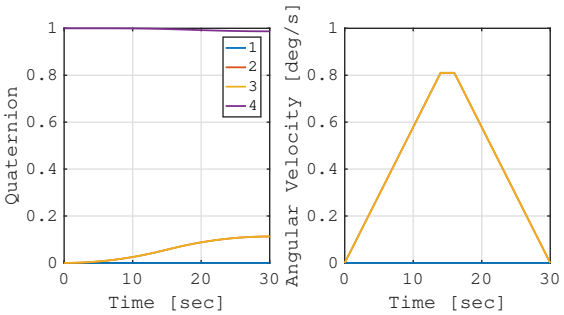

Fig. 4.: Reference trajectories of the quaternion and the angular velocity in the case A

For an example, the reference trajectories for the case A are shown in the Fig. 4. The large reference angular velocity like the case C requires large torque and therefore gimbals are steered rapidly. In this case, the control inputs exceeding the gimbal rate limitations are often calculated and the singularity passage should be conducted.

Simulation results of the case A are shown in the Fig. 5. In order to make it easy to evaluate the attitude error, only first, second and third elements of the error quaternion are shown. It is found that the proposed method evaluates that the avoidance has smaller attitude error than the passage and it avoids the singular state. The decision is right judging from the quite small error angle shown in the figure. Also, as we expected in the section 3, the figure shows that the outer gimbal rate dramatically increases when $\theta_i \approx \pi/2$.

Simulation results of the case B are shown in the Fig. 6. In this cases, the evaluation functions become

$$L^+ = 1.90 \times 10^{-3}, L^- = 1.82 \times 10^{-3}$$

at $t = 3.2$ s and the passage (transition of the solution) starts. For comparison, the case is shown in the Fig. 7 where the Eq. (18)–(20) is always selected, namely, the avoidance is compulsorily conducted. These figures show that the avoidance has slightly smaller attitude error than the avoidance. As the evaluation function employed in the proposed method is just an approximation, it is found that the decision might be wrong when L^+ and L^- are nearly equal. However, these figures also show that the attitude error does not make much difference in two cases and such a wrong decision is not a problem in practice.

Simulation results of the case C are shown in the Fig. 8. In this case, the passage can decrease more attitude error than the avoidance, and the algorithm rightly recognizes it and starts to pass the singular state at $t = 1.9$ s. As with the case B2, the case of the compulsory avoidance is shown in the Fig. 9. This figure shows that the attitude error becomes large due to the significant violation of the gimbal rate limitation when the singular state is avoided, as we expected in the section 3. From the results above, it is shown that the proposed steering logic can estimate the cost of the singularity avoidance/passage and select the action which causes the small attitude error.

Next, we will evaluate torque error defined as the difference between the output and reference torque. This is because the proposed method does not use any correction term for the singularity avoidance and is expected to be able to generate precise torque close the reference torque. We compare the torque error in our method with that in the Tsukahara's method[6] in the case A. The parameters for the singularity avoidance employed in the Tsukahara's method is specified as

$$\delta = 0.2, \quad l = 0.2$$

Simulation results are shown in the Fig. 10. The Tsukahara's method has the error of approximately -1.7×10^{-2} Nm at maximum. On the other hand, the error in the proposed method is less than -2.4×10^{-3}Nm and this results show that the proposed steering logic can generate precise torque.

5. Conclusion

In this paper, we proposed a novel singularity avoidance/passage logic based on inverse kinematics for steering a VSDGCMG. This method does not employ any correction term, which is for the singularity avoidance and required in the previously proposed steering logic, and it can generate a precise torque close to the reference torque. Also, it uses an evaluation function including gimbal rate limitations explicitly for the singularity avoidance/passage decision. This function leads a decision causing small attitude-error compared with the previous method which uses a simple threshold. Effectiveness of the method was demonstrated by the numerical simulations.

Acknowledgments

This work was supported by JSPS KAKENHI Grant Number 26289329.

References

1) Ishizaka, K., Matunaga, S. and TSUBAME development team: Design and development of the Earth and astronomical observation technology demonstration satellite -TSUBAME-, 8th IAA Symposium on Small Satellites for Earth Observation, Berlin, Germany, IAA-B8-0316P, April 2011.
2) Funase, R. et al.: One-year Deep Space Flight Result of the World's First Full-scale 50kg-class Deep Space Probe PROCYON and Its Future Perspective, 30th Annual AIAA/USU Conference on Small Satellite, Utah, US, SSC16-III-05, Aug. 2016.
3) Stevenson, D. and Schaub, H.: Nonlinear Control Analysis of a Double-Gimbal Variable-Speed Control Moment Gyroscope, *Journal of Guidance, Control, and Dynamics*, **35**, 3 (2012), pp.787–793.
4) Zhang, H. and Fang, J.: Robust Backstepping Control for Agile Satellite Using Double-Gimbal Variable-Speed Control Moment Gyroscope, *Journal of Guidance, Control, and Dynamics*, **36**, 5 (2013), pp.1356–1363.
5) Jikuya, I., Fujii, K. and Yamada, K.: Attitude maneuver of spacecraft with a variable-speed double-gimbal control moment gyro, *Advances in Space Research*, **58**, 7 (2016), pp. 1303–1317.
6) Tsukahara, T., Yamada, K. and Shoji, Y.: On the Singularity Avoidance/Passage Law of a Variable-speed Double-gimbal Control Moment Gyro , *Aerospace Technology*, **15** (2016), pp. 53–61 (in Japanese).
7) Yamada, K., Asai, T. and Jikuya, I.: Inverse Kinematics in Pyramid-Type Single-Gimbal Control Moment Gyro System, *Journal of Guidance, Control, and Dynamics*, **39**, 8 (2016), pp. 1897–1907.

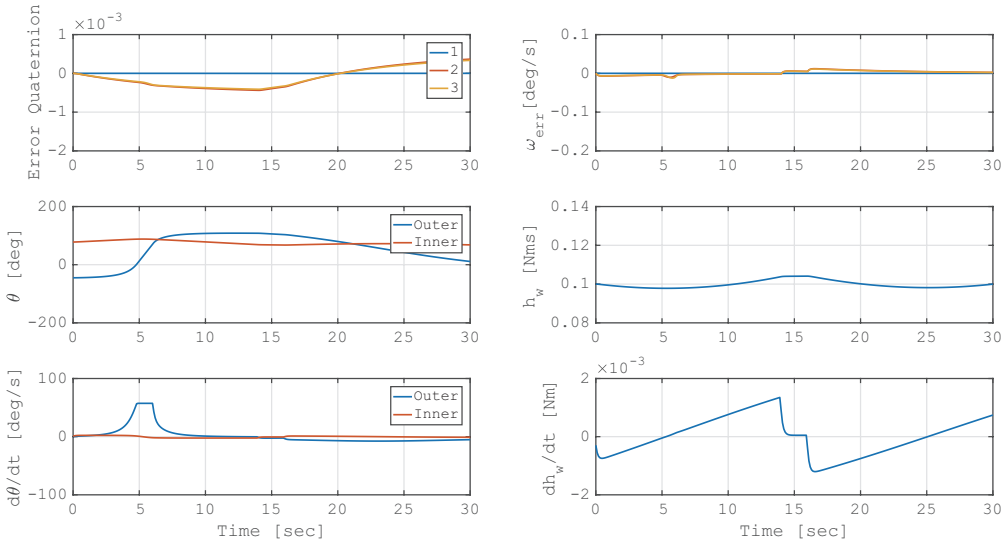

Fig. 5.: Case A (avoidance).

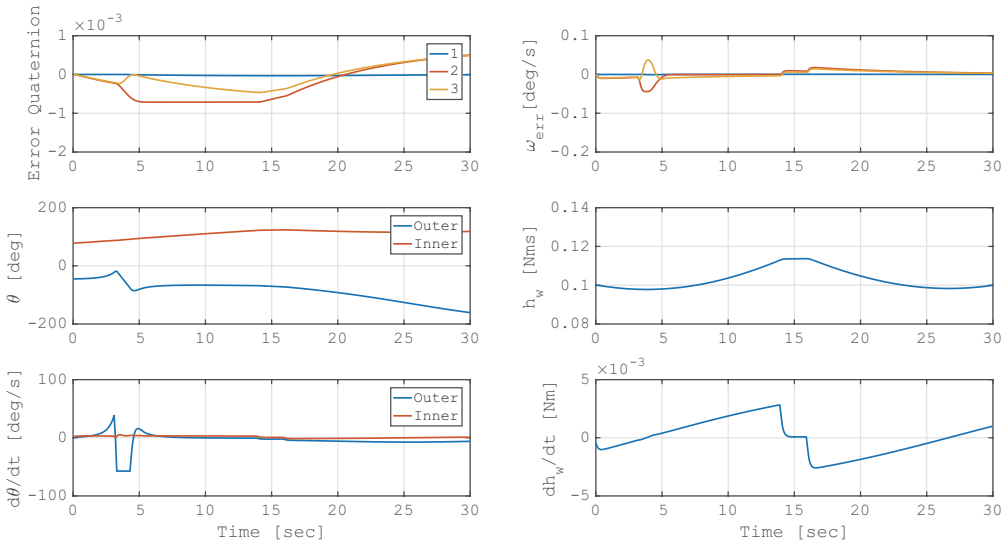

Fig. 6.: Case B (passage).

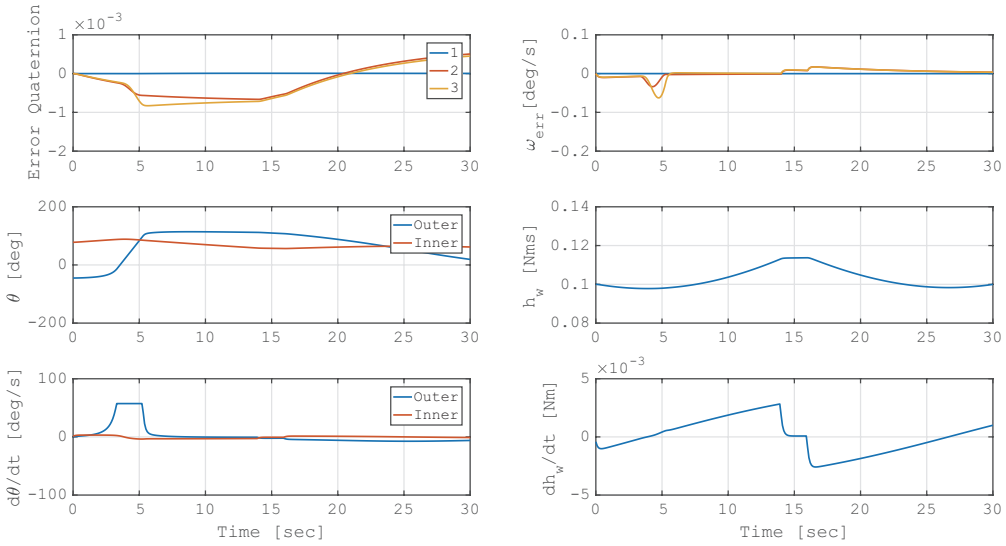

Fig. 7.: Case B2 (compulsory avoidance).

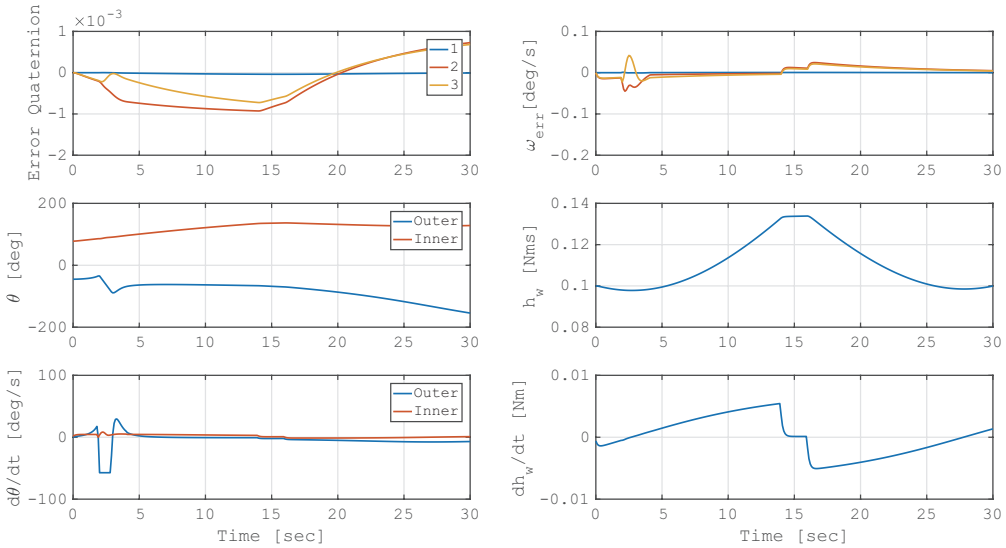

Fig. 8.: Case C (passage).

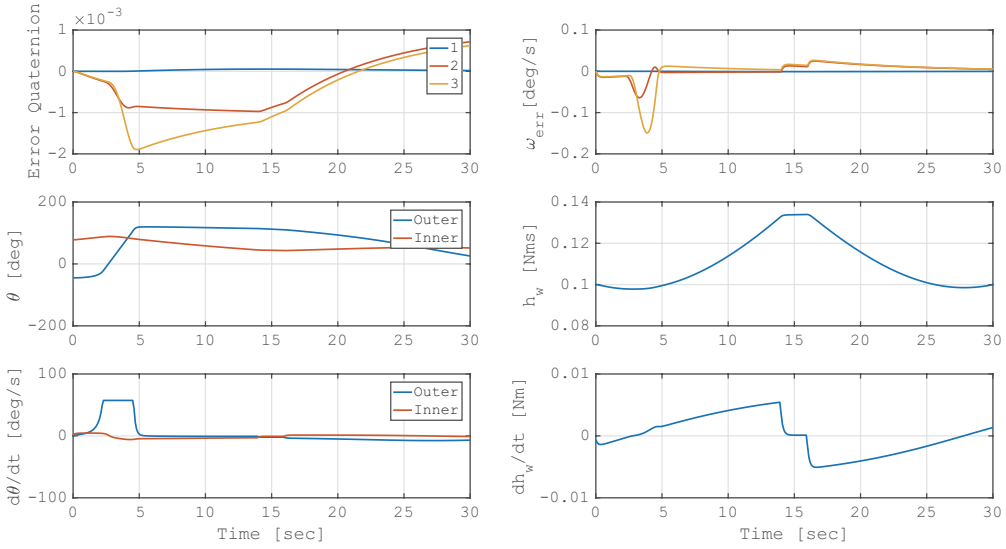

Fig. 9.: Case C2 (compulsory avoidance).

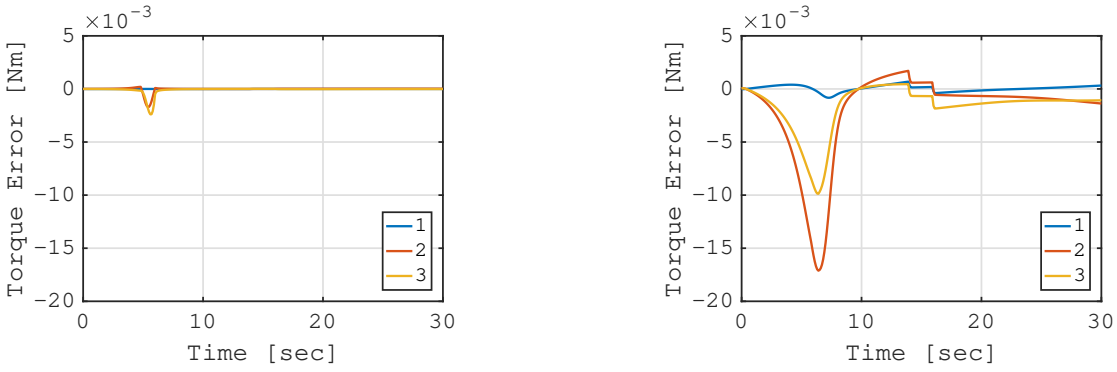

(a) Proposed method

(b) Tsukahara's method

Fig. 10.: Time history of torque error in the case A